Sound Attenuation by a Two-Dimensional Array of Rigid Cylinders

J. V. Sánchez-Pérez,[1] D. Caballero,[2] R. Mártinez-Sala,[1] C. Rubio,[1] J. Sánchez-Dehesa,[2,*] F. Meseguer,[1,3,*] J. Llinares,[1] and F. Gálvez[1]

[1]*Unidad Asociada Consejo Superior de Investigaciones Científicas, Departamento de Física Aplicada, Universidad Politécnica de Valencia, Camino de Vera, E-46022 Valencia, Spain*

[2]*Departamento de Física Teórica de la Materia Condensada, Facultad de Ciencias (C-5), Universidad Autónoma de Madrid, E-28049 Madrid, Spain*

[3]*Instituto de Ciencia de Materiales, Consejo Superior de Investigaciones Científicas, Campus de Cantoblanco, E-28049 Madrid, Spain*

(Received 26 February 1998)

In this Letter we present an experimental analysis of the acoustic transmission of a two-dimensional periodic array of rigid cylinders in air with two different geometrical configurations: square and triangular. In both configurations, and above a certain filling fraction, we observe an overlap, in the range of the audible frequencies, between the attenuation peaks measured along the two high-symmetry directions of the Brillouin zone. This effect is considered as the fingerprint of the existence of a full acoustic gap. Nevertheless, the comparison with our calculation of band structures shows that the triangular lattice has band states in that frequency range. We call them *deaf bands*. This contradictory result is explained by looking at the symmetry of the deaf bands; they cannot be excited by experiments of sound transmission. [S0031-9007(98)06295-4]

PACS numbers: 43.20.+g, 42.25.Bs, 52.35.Dm

In the late 1980s, several authors [1,2] showed that a transparent material can become opaque for any light wave vector provided that a strong modulation of the refractive index in the three dimensions of the space is attained. These systems were called photonic-band-gap (PBG) materials because of the analogy to the behavior of electrons in crystals; in the same manner as electrons are allowed in certain energy bands, photons in PBG materials can exist only in certain frequency bands.

One of the advantages of PBG materials is that the underlying theory can be applied to other types of waves like sound or elastic waves [3]. The crucial parameter that allows the appearance of gaps in PBG materials is the ratio between the dielectric constant in the scatterers and in the host. For sound and elastic waves two parameters determine the gaps: the density and the velocity ratio. A great effort has already been put in the theoretical study of these kinds of waves [4–6]. To the best of our knowledge, the experimental studies of band-gap materials based on classical waves are mostly restricted to electromagnetic waves. Some of us showed that some minimalist sculptures have properties of sound-band-gap materials [7]. This work has stirred interest [8,9] about whether this sort of structure presents full band-gap effects. Also, experiments performed in two-dimensional composite materials have been reported that show localization of bending waves [10], and the formation of ultrasonic full band gap [11].

The goal of this Letter is the experimental study of the sound attenuation by two-dimensional (2D) periodic distributions of sound scatters in air with square and triangular arrangements. We also present a theoretical calculation of the acoustic bands that allows the interpretation of the experimental observations.

The experiments have been performed in an anechoic chamber. The dimension of the chamber ($8 \times 6 \times 3\ m^3$) is not much larger than the sample size. Therefore, sound waves are not full plane waves when the wave fronts reach the samples. The samples, that we call minimalist sculptures, are build up by hanging cylindrical bars on a frame with square or triangular symmetry. The frame can rotate around the vertical axis, so one can explore any direction of the **k** wave vector perpendicular to the cylinder axis. We used hollow and full stainless steel cylinders as well as wood cylinders, the results being practically independent of this factor. Cylinders with diameter $d = 1$, 2, 3, and 4 cm, respectively, have been parallelly arranged in square configurations with lattice constant $a = 5.5$ and 11 cm, respectively. For triangular configurations the lattice constant was 6.35 and 12.7 cm. The change of the parameters, a and d, allowed us to study filling fractions of volume occupied by cylinders ranging from 0.006 up to 0.41 for the square symmetry, and 0.005 up to 0.36 for triangular symmetry. We have built up sculptures with a finite number, N, of elements; from 100 to 500 elements. The results obtained show that the location of the Bragg peak for the diffraction is independent of N, while the attenuation intensity increases with N. We use a sound source B & K 4204 and two microphones, one as a reference and the second one to detect the sound transmitted through the sculpture. A dual channel signal analyzer type B & K 2148 has been used through all the experiments.

To perform the theoretical calculation we have considered infinite cylinders along the z axis. We have to solve

the following eigenvalue equation for the pressure waves $p(\mathbf{r})$ in the 2D space $\mathbf{r} = (x, y)$:

$$\nabla \cdot \left(\frac{\nabla p(\mathbf{r})}{\rho(\mathbf{r})} \right) = -\omega^2 \frac{p(\mathbf{r})}{c^2(\mathbf{r})\rho(\mathbf{r})}, \tag{1}$$

where ω is the frequency of a harmonic eigenmode, and $c(\mathbf{r})$ and $\rho(\mathbf{r})$ are the sound velocity and the density, respectively, that are dependent on the position.

Since the systems are periodic, the Bloch's theorem asserts that $p(\mathbf{r})$ is of the form $p(\mathbf{r}) = p_{n,\mathbf{k}}(\mathbf{r}) = u_{n,\mathbf{k}}(\mathbf{r}) e^{i\mathbf{k}\cdot\mathbf{r}}$, where $u_{n,\mathbf{k}}(\mathbf{r})$ is a function with the same periodicity as the underlying lattice. The usual approach to solve this equation is the plane-wave (PW) method [8,9]. Here, we employ a novel variational method developed by us. In this method the pressure is expanded as a superposition of a finite number M of localized functions $\phi_i(\mathbf{r})$:

$$p_{n,\mathbf{k}}(x, y) = \sum_{i=1}^{M} b_i \sum_{\mathbf{R}} e^{i\mathbf{k}\cdot\mathbf{R}} \phi_i(\mathbf{r} - \mathbf{R}). \tag{2}$$

$\mathbf{R}$ defines the Bravais lattice of the system. Each localized function $\phi_i(\mathbf{r})$ is a product of one-dimensional cubic B splines, i.e., piecewise C^2-smooth cubic polynomials [12]. Plugging expansion (2) in the wave equation (1) produces the following matrix equation:

$$[\mathcal{A}(\mathbf{k}) + \omega_n^2(\mathbf{k})\mathcal{E}(\mathbf{k})]\mathbf{b} = \mathbf{0}, \tag{3}$$

where the matrix elements are

$$\mathcal{A}_{ij}(\mathbf{k}) = \int \phi_i(\mathbf{r}) \mathcal{A} \phi_j(\mathbf{r})\, d\mathbf{r} + \sum_{\mathbf{R}} e^{i\mathbf{k}\cdot\mathbf{R}} \int \phi_i(\mathbf{r}) \mathcal{A} \phi_j(\mathbf{r} - \mathbf{R})\, d\mathbf{r} + \sum_{\mathbf{R}} e^{-i\mathbf{k}\cdot\mathbf{R}} \int \phi_i(\mathbf{r} - \mathbf{R}) \mathcal{A} \phi_j(\mathbf{r})\, d\mathbf{r}, \tag{4}$$

$$\mathcal{E}_{ij}(\mathbf{k}) = \int \phi_i(\mathbf{r}) \mathcal{E} \phi_j(\mathbf{r})\, d\mathbf{r} + \sum_{\mathbf{R}} e^{i\mathbf{k}\cdot\mathbf{R}} \int \phi_i(\mathbf{r}) \mathcal{E} \phi_j(\mathbf{r} - \mathbf{R})\, d\mathbf{r} + \sum_{\mathbf{R}} e^{-i\mathbf{k}\cdot\mathbf{R}} \int \phi_i(\mathbf{r} - \mathbf{R}) \mathcal{E} \phi_j(\mathbf{r})\, d\mathbf{r} \tag{5}$$

and $\mathbf{b}$ is a matrix column with the coefficients b_i.

It can be demonstrated that operators $\mathcal{A} = \nabla \cdot (\frac{\nabla}{\rho})$, and $\mathcal{E} = \frac{1}{c^2\rho}$ are self-adjoints. The resulting matrices are Hermitian and sparse, and specially designed routines [13] are used to solve Eq. (3). Notice that the method is variational, the coefficients b_i being the variational parameters. Therefore a sufficient number of localized functions must be employed to guarantee the convergence

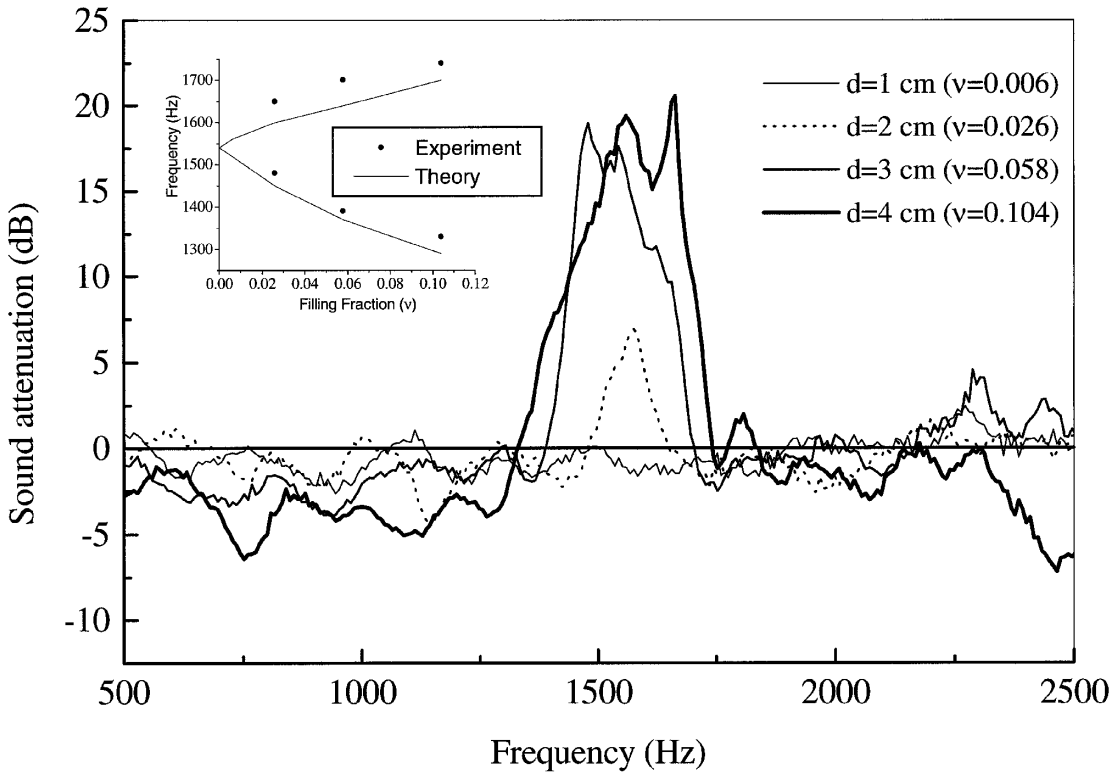

FIG. 1. Attenuation spectra for acoustic waves incident along the ΓX direction (i.e., along [100]) in different square arrangements of rigid cylinders in air. The lattice constant is 11 cm. Each sculpture sample differs in the diameter d of the cylinders. ν is the filling fraction. The inset shows the comparison between the limits of the attenuation peak observed (full dots) and band gap calculated (continuous lines).

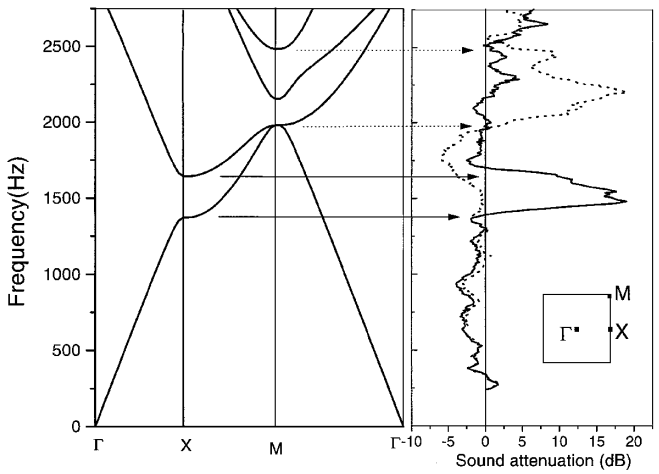

FIG. 2. Sound attenuation vs frequency for an arrangement of rigid cylinders of diameter 3 cm in a square lattice with periodicity 11 cm. The arrows indicate the limits of the gaps calculated (right panel). Acoustic bands calculated by our variational method for the sculpture sample described above (left panel).

of the numerical results. 100 functions are enough to get results comparable to those obtained by the PW method. In what follows we will describe the results obtained using a velocity and density ratio of 17.2 and 2069, respectively, corresponding to stainless steel rigid cylinders in air.

In Fig. 1 we show the attenuation spectra of different square lattice samples taken for acoustic waves with **k** vectors along the ΓX direction. The inset shows the comparison between theoretical and experimental band-gap edges of the first acoustic gap at the X point of the Brillouin zone (BZ). The agreement between theory and measurements is fairly good in view of the finite dimension of the sculpture samples.

In Fig. 2 we plot the spectra for the case of cylinders of diameter 3 cm in a square lattice with periodicity of 11 cm and the corresponding band structure. At the X point the first calculated gap appears in a frequency region (1.37–1.64 kHz) in close agreement with the experimental attenuation peak (1.38–1.70 kHz). Regarding the attenuation peak observed along the ΓM direction (1.97–2.56 kHz), the theory predicts the existence of two bands in this range of frequencies (the second and third bands in Fig. 2) that would produce the transmission of sound.

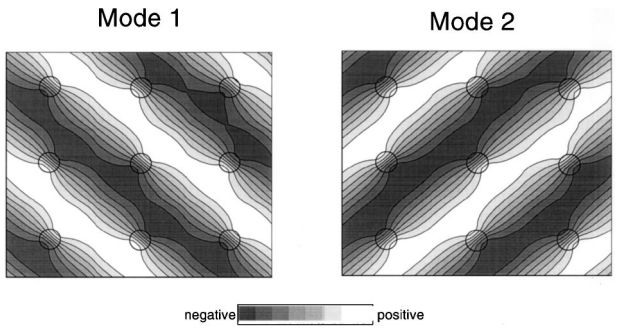

FIG. 3. Pressure field of band-edge states inside a square array of rigid cylinders in air. The grey scale indicates the amplitude of the pressure field. Modes are shown near the M point belonging to bands 1 and 2 of Fig. 2. Mode 1 has the appropriate symmetry to be excited by a plane-wave incident along the ΓM direction (i.e., along the [110] direction). On the contrary, mode 2 cannot be excited by such a wave and it is *deaf* to the incident sound.

This apparently strange behavior can be explained by the particular symmetry of the states. Physically, we can figure out this effect by looking at the pressure field pattern of the eigenmodes plotted in Fig. 3. This figure shows the two modes with lowest frequencies near the M point of the first BZ. While mode 1 has the proper symmetry to be excited by an incident plane wave traveling along the [110] direction, mode 2 has the planes of equal phase along the perpendicular direction and consequently cannot be excited by such a wave. We call the latter mode *deaf*, in a manner similar to that reported by other authors for the case of two-dimensional PBG materials [14,15]. In effect, when we discard the *deaf bands* the resulting effective gap (1.98–2.58 kHz) practically coincides with the attenuation peak measured.

Notice that spectra of Fig. 2 do not coincide with previous measurements reported by some of us in open air [7]. The sound could be reflected in the surrounding buildings. The resulting wave vector mixing produces a sound attenuation spectrum **k**-vector independent.

For triangular arrangements, Table I shows the range of frequencies at which the attenuation band appears along the ΓX direction for all the systems analyzed. Attenuation peaks with bandwidths below 0.24 kHz are not detected due to experimental accuracy. Along the ΓM direction an effect, induced by the existence of deaf

TABLE I. Summary of results for the first attenuation gap along the ΓX direction for an array of rigid cylinders in air with triangular symmetry.

Lattice constant (cm)	Cylinder diameter (cm)	Filling fraction (ν)	$X_1 \rightarrow X_2$ measured (kHz)	$X_1 \rightarrow X_2$ calculated (kHz)
6.35	1	0.022	Not observed	2.94 → 3.18
6.35	2	0.089	2.84 → 3.30	2.66 → 3.33
6.35	3	0.202	2.39 → 3.33	2.40 → 3.44
6.35	4	0.360	2.16 → 3.30	2.22 → 3.37
12.7	1	0.006	Not observed	1.52 → 1.56
12.7	2	0.022	Not observed	1.47 → 1.59
12.7	3	0.051	1.35 → 1.64	1.40 → 1.63
12.7	4	0.089	1.30 → 1.67	1.32 → 1.67

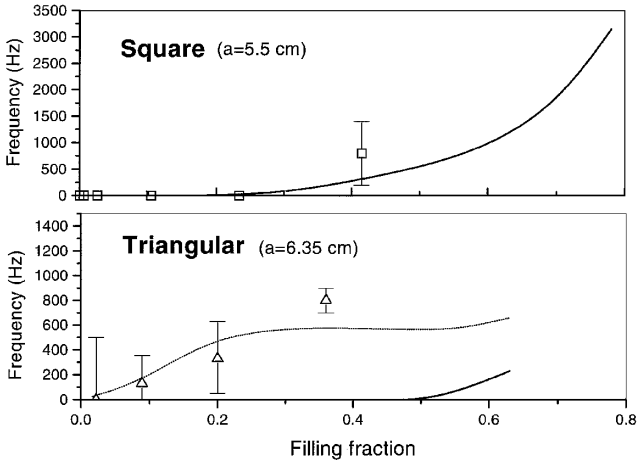

FIG. 4. The full lines represent the calculated gap widths of the lowest stop-band for the two configurations of rigid cylinders in air analyzed. The symbols define the acoustic gap obtained from transmission experiments. For the triangular case, the dotted line gives the effective acoustic gap calculated with the exclusion of the *deaf bands* (the ones not accessible by symmetry for the incident sound).

bands, appears, as described before. Now, there is an overlap between the attenuation peaks measured along ΓX and ΓM directions, respectively, although states (the deaf bands) are present. Therefore, an effective acoustic gap can be defined that is different from the full band gap theoretically calculated. This experimental fact has important consequences since the full band gap, defined by the absence of states in the frequency region, theoretically appears for filling fractions much larger than experimentally found.

To conclude, in Fig. 4 we show the summary of the results regarding the lowest gap of the sound attenuation. The continuous lines represent the calculated width of the full band gap. The width of the acoustic gap experimentally observed is described by full squares (full triangles) for the square symmetry (triangular symmetry). It can be observed that for the sculptures with square symmetry the agreement between theory and experiment is fairly good. Nevertheless, for the samples with triangular symmetry such agreement exists only if the comparison is done with an effective acoustic gap (dashed line), rather than with the absolute band gap. The former is calculated so that the deaf bands are not taken into account for the sound propagation. At this point, let us stress that the existence of deaf bands in the dispersion relation is beyond doubt, but we found that experiments like the ones described here are not capable to detect them. Moreover, notice that this peculiar property has important implications since the noise of certain frequencies could be stopped by a specially designed finite array of cylinders although a full band gap does not exist in the same range of frequencies.

In summary, we have experimentally studied the attenuation of sound by square and triangular arrays of rigid cylinders in air. We have been able to get a full acoustic band gap in the range of audible frequencies for the systems of square symmetry with a filling fraction of 0.41. The comparison with our calculation of the band structure is very good and has allowed us to identify deaf bands for the sound transmission in the dispersion relation. As a consequence, we have shown that, for the case of triangular symmetry, an effective acoustic gap is observed in a range of frequencies where theory does not predict full band gap. These findings can be exploited to design acoustic screens or filters, based on the existence of deaf bands.

This work has been supported by the Comision Interministerial de Ciencia y Tecnología of Spain, Contract No. MAT97-0698-C04, and the Generalitat Valenciana, Contract No. GV-D-CN-08-129-96. We thank Cefe López for a critical reading of the manuscript.

*Authors to whom correspondence should be addressed. Electronic addresses: jsdehesa@uamca3.fmc.uam.es, fmese@fis.upv.es

[1] E. Yablonovitch, Phys. Rev. Lett. **58**, 2059 (1987).
[2] S. John, Phys. Rev. Lett. **58**, 2486 (1987).
[3] E. N. Economou and M. Sigalas, *Photonic Band Gaps and Localization*, edited by C. M. Sokoulis (Plenum Press, New York, 1993).
[4] M. M. Sigalas and E. N. Economou, J. Sound Vib. **158**, 377 (1992).
[5] M. S. Kushwaha, P. Halevi, L. Dobrzynski, and B. Djafrari-Rouhani, Phys. Rev. Lett. **71**, 2022 (1993).
[6] E. N. Economou and M. Sigalas, Phys. Rev. B **18**, 13 434 (1993).
[7] R. Mártinez-Sala, J. Sancho, J. V. Sánchez, V. Gómez, J. Llinares, and F. Meseguer, Nature (London) **378**, 241 (1995).
[8] M. M. Sigalas and E. N. Economou, Europhys. Lett. **36**, 241 (1996).
[9] M. S. Kushwaha, Appl. Phys. Lett. **70**, 3218 (1997).
[10] L. Ye, G. Cody, M. Zhou, and P. Sheng, Phys. Rev. Lett. **69**, 3080 (1992).
[11] F. R. Montero de Espinosa, E. Jiménez, and M. Torres, Phys. Rev. Lett. **80**, 1208 (1998).
[12] C. de Boor, *A Practical Guide to Splines* (Springer, New York, 1978).
[13] We use the routine nag-sym-gen-eigsel taken from the NAG-fl90 library.
[14] W. M. Robertson, G. Arjavalingam, R. D. Meade, K. D. Brommer, A. M. Rappe, and J. D. Joannopoulos, Phys. Rev. Lett. **68**, 2023 (1992).
[15] T. F. Krauss, R. M. de la Rue, and S. Brand, Nature (London) **383**, 699 (1996).